Seasonal Variation and Sources of Carbonaceous Species and Elements in PM2.5 and PM10 Over the Eastern Himalaya

Sudhir Kumar Sharma (sudhir@nplindia.org)
CSIR-National Physical Laboratory, Dr. K. S. Krishnan Road, New Delhi-110 012, India
https://orcid.org/0000-0003-2268-3933

Sauryadeep Mukherjee
Bose Institute

Nikki Choudhary
CSIR-National Physical Laboratory: National Physical Laboratory CSIR

Akansha Rai
CSIR-NPL: National Physical Laboratory CSIR

Abhinandan Ghosh
Bose Institute

Abhijit Chatterjee
Bose Institute

Narayanswami Vijayan
CSIR-National Physical Laboratory: National Physical Laboratory CSIR

Tuhin Kumar Mandal
CSIR-National Physical Laboratory: National Physical Laboratory CSIR

Research Article

Keywords: PM2.5, PM10, OC, EC, WSOC, Elements, PCA

Posted Date: February 9th, 2021

DOI: https://doi.org/10.21203/rs.3.rs-168623/v1

Seasonal variation and sources of carbonaceous species and elements in $PM_{2.5}$ and PM_{10} over the eastern Himalaya

Sudhir Kumar Sharma[1,2*] • Sauryadeep Mukherjee[3] • Nikki Choudhary[1,2] • Akansha Rai[1,2] • Abhinandan Ghosh[3] • Abhijit Chatterjee[3] • Narayanswami Vijayan[1] • Tuhin Kumar Mandal[1,2]

[1]CSIR-National Physical Laboratory, Dr. K. S. Krishnan Road, New Delhi-110 012, India.

[2]Academy of Scientific and Innovative Research (AcSIR), Ghaziabad-201 002, India

[3]Centre for Astroparticle Physics and Space Sciences, Bose Institute, Darjeeling-734 102, India.

* Author's to Correspond:

Sudhir Kumar Sharma

Environmental Sciences and Biomedical Metrology Division
CSIR-National Physical Laboratory
Dr. K S Krishnan Road
New Delhi-110 012, India
E-mail: sudhir.npl@nic.in; sudhircsir@gmail.com
Phone: +91-11-45609448
Fax: +91-11-45609310

Abstract

The study represents the seasonal characteristics (carbonaceous aerosols and elements) and contribution of prominent sources $PM_{2.5}$ and PM_{10} in the high altitude of the eastern Himalaya (Darjeeling) during August 2018-July 2019. Carbonaceous aerosols [organic carbon (OC), elemental carbon (EC) and water soluble organic carbon (WSOC)] and elements (Al, Fe, Ti, Cu, Zn, Mn, Cr, Ni, Mo, Cl, P, S, K, Zr, Pb, Na, Mg, Ca, and B) in $PM_{2.5}$ and PM_{10} were analyzed to estimate their possible sources. The annual average concentration of $PM_{2.5}$ and PM_{10} were computed as 37±12 μg m^{-3} and 58±18 μg m^{-3}, respectively. In the present case, total carbonaceous species in $PM_{2.5}$ and PM_{10} were accounted for 20.6% of $PM_{2.5}$ and 18.6% of PM_{10}, respectively. Whereas, trace elements in $PM_{2.5}$ and PM_{10} were estimated as 15% of $PM_{2.5}$ and 12% of PM_{10}, respectively. Monthly are seasonal variations in concentrations of carbonaceous aerosols and elements in $PM_{2.5}$ and PM_{10} were also observed during the observational period. The positive relationship between OC & EC and OC & WSOC of $PM_{2.5}$ and PM_{10} during all the seasons (except monsoon in case of PM_{10}) indicate rheir common sources. The enrichment factors (EFs) and significant positive correlation of Al with othe crustal elements (Fe, Ca, Mg and Ti) of fine and coarse mode aerosols indicates the influence of mineral dust at the Darjeeling. Principal component analysis (PCA) resolved the four common sources (biomass burning + fossil fuel combustion (BB+FFC), crustal/soil dust, vehicular emissions (VE) and industrial emissions (IE)) of $PM_{2.5}$ and PM_{10} in Darjeeling.

Keywords: $PM_{2.5}$, PM_{10}, OC, EC, WSOC, Elements, PCA

1. Introduction

The urban agglomeration of hilly region of India is under serious threat various forms of anthropogenic activities and pollutants (Gajananda et al. 2005; Sharma et al. 2020a;b). Due to rapid urbanization, industrialization, increasing vehicular traffic due to increased tourism-related activities, increase in energy demands (for lighting, cooking and heating etc.) have resulted in contamination/deterioration of ambient air quality, vegetation and climate of the hilly region (Chatterjee et al. 2010; Rai et al. 2020a). From last few decades the fine and coarse mode of aerosol/particulate matter (PM) has been altered the atmospheric particle chemistry, Earth's climate system (radiative balance), and human health (Pant and Harrison 2012; Bond et al. 2013). Therefore, quantification and identification of chemical species and sources of aerosol is essential to explore the appropriate mitigation option to improve the ambient air quality, human health and climate (Ramana et al. 2010; Cao et al. 2006; Bond et al. 2013; Pope et al. 2009; Ramgolam et al. 2009; Sharma et al. 2018 a; b; Rai et al., 2020b).

Carbonaceous aerosols (CAs) are the major fractions (OC, and EC) of $PM_{2.5}$ and PM_{10} in the atmosphere and have significant role in the Earth's radiative balance, visibility degradation, alteration of atmospheric chemistry (Lim and Turpin 2002; Hansen et al. 2005; Bond et al. 2013; Pope et al. 2009). Various toxic gases (CO, CO_2, SO_x, NH_3, and NOx, etc.,) organics and hydrocarbons (like, VOCs: volatile organic compounds; PAHs: polycyclic aromatic hydrocarbons) are produced during the combustion process/emissions of CAs and therefore affect the respiratory/cardiovascular system of the human (Lighty et al. 2000; Pope et al. 2009). Both primary and secondary organic aerosols significantly control of physico-chemical properties of particles/aerosols (Kanakidou et al. 2005) and influenced the formation cloud condensation nuclei (CCN), whereas EC absorb solar radiation and contribute for radiative change (Bond et al., 2013).

PM consists of organics (OC, EC, and other components), mineral/crustal/soil dust, metals, non-metals, inorganic pollutants as well as sea salts and relative exuberance of these components are highly variable both spatially and temporally (Ram et al. 2011; Jain et al. 2017). Generally, the elements linked with the PM are non-volatile in nature and remain unaffected even though they go for regional as well as long-range transportation (Morawska and Zhang, 2002). Some of the transition/toxic metals (like Fe, Cu, Mn, Zn, Ni, Cr, As, Pb, Hg) which are coming from the various sources into the ambient air have acute toxic and mutagenic effects on human health, when inhaled at higher concentrations. Elements like Fe, Al, Si, Ca and Ti are also available in the fine and coarse mode PM is originated from mineral dust/crustal dust (Sharma et al. 2014a). Soluble K in PM mostly originated

from biomass burning, however, it is also attributed to dust in PM (Viana et al. 2008), whereas Cl originated from sea salt is also considered from coal burning in aerosols (Pant and Harrison 2012).

Several studies conducted in past on carbonaceous aerosols, inorganic aerosols and elements in particulate matter and their potential sources in urban (Ram and Sarin, 2011; Mandal et al. 2014; Sharma et al. 2016; Gupta et al. 2018; Shivani et al. 2019; Jain et al. 2020a;b), rural, remote (Begam et al. 2017) as well as high altitude atmosphere (Ram et al. 2008; Kumar and Attri, 2016; Sarkar et al. 2017; Kaushal et al. 2018) but very limited study (Sharma et al. 2020b) has been conducted in the eastern Himalayan region of India. Considering the importance of atmospheric carbonaceous species and elements in $PM_{2.5}$ and PM_{10} and from their perspective on climate change, the present study has been carried out at Darjeeling (the eastern Himalaya). In this paper, we report the carbonaceous components (OC, EC, and WSOC) and elements (Al, Fe, Ti, Cu, Zn, Mn, Cr, Ni, Mo, Cl, P, S, K, Zr, Pb, Na, Mg, Ca, and B) of $PM_{2.5}$ and PM_{10} over the eastern Himalaya (Darjeeling) during August 2018 – July 2019. Principal component analysis (PCA) and HYSPLIT trajectory were applied to resolve the potential sources and source region, respectively of $PM_{2.5}$ and PM_{10} at Darjeeling.

2. Materials and methods

2.1 Description of study site

The study was carried out in the campus of Bose Institute, Darjeeling (27.01 ºN and 88.15ºE; 2200 m asl) situated in the Eastern Himalaya (Fig. 1). The hilly districts of Darjeeling are situated within the lower and sub-Himalayan ranges of the eastern Himalaya. Darjeeling is surrounded by Sikkim Himalayas, Bhutan Himalaya and Nepal Himalaya from the north, east and west sides, respectively (Chatterjee et al. 2021). The study area is considered as a semi-urban and is under he influence of biomass burning, vehicle emissions, agriculture and tourism activities (Adak et al. 2014). The climate of Darjeeling is subtropical and temperate with wet summer/pre-monsoon and monsoonal rains (June-September). The annual average maximum temperature was estimated to be 12.2 °C (in summer: March-May) whereas the average minimum temperature was estimated as 3.4 °C (in winter: January-February) with monthly mean temperatures ranging from 5.8 to 17.2 °C. The monthly average meteorology (ambient temperature, relative humidity (RH), wind speed and wind directions) during the study period are depicted in Fig. S1 (see the supplementary information). The detail information on topography, weather, township and influences of local pollution sources at the study site is described in Chatterjee et al. (2021).

105

106 **2.2 Sample collection and analysis**

107 $PM_{2.5}$ (n = 94) and PM_{10} (n = 102) samples were collected simultaneously on pre-combusted (at 550 °C)
108 Pallflex tissue quartz filters (47mm for $PM_{2.5}$ and 20×25 cm^2 for PM_{10}) using Fine Particle Sampler (flow rate: 1m^3
109 h^{-1} ± 2 %) and Respirable Particle Sampler (flow rate:1.2 m^3 min^{-1} ± 2 %), respectively for 24h from August 2018-
110 July 2019 ($PM_{2.5}$ sampling was not carried out in July 2019). The particle sampler was placed on the rooftop of the
111 Bose Institute at the height of 15m above the ground level. The gravimetric mass (in µg) of $PM_{2.5}$ and PM_{10} was
112 computed by the difference between the initial and final weight using a calibrated weighing balance (M/s. Sartorius,
113 resolution: ± 10 µg) of the filter. The concentrations of $PM_{2.5}$ and PM_{10} (in µg m^{-3}) were further computed by
114 dividing the PM mass to the total volume of air passed during the sampling period (24h). Before chemical analysis
115 the samples were stored at −20ºC.

116 The concentrations of OC and EC in $PM_{2.5}$ and PM_{10} samples were estimated by OC/EC Carbon analyzer
117 (Model: DRI 2001A; Make: Atmoslytic Inc., Calabasas, CA, USA) using IMPROVE-A Protocol (Chow et al.
118 2004). OC/EC carbon analyzer is working on the preferential oxidation of OC and EC at different temperatures
119 plateaus (140, 280, 480 and 580°C; for OC1, OC2, OC3 and OC4, respectively) in pure helium and three
120 temperature plateaus (580, 740 and 840°C for EC1, EC2 and EC3, respectively) in 98 % helium and 2 % oxygen
121 (Chow et al. 2004). A proper punch of ~0.536 cm^2 area of the filter was cut and analyzed in triplicate along with
122 field blank filters. The standard calibration for peak area verification was performed daily using 5% CH_4+balance
123 helium gas (before and after sample analysis). Calibration of the OC/EC analyzer was performed by 4.8% of CO_2 +
124 balance He gas along with known amounts of KHP (potassium hydrogen phthalate) and sucrose solution (Sharma et
125 al. 2020b). In the present case, repeatability error of OC and EC analysis were estimated as 3-7% (n=3). Total
126 carbonaceous aerosols (TCA) of $PM_{2.5}$ and PM_{10} are computed as (1.6×OC)+EC (Rengarajan et al. 2007; Srinivas
127 and Sarin 2014).

128 A known punch size of $PM_{2.5}$ (~3.46 cm^2) and PM_{10} (~7.07 cm^2) filters were cut into four halves and was
129 soaked in 20 ml of de-ionized water (18.2 MΩ-cm) and ultrasonicated three times for 10 min each. The 10ml filtered
130 extract was transferred into a pre-cleaned glass vial and analyzed for WSOC and WIOC using a TOC analyzer
131 operating on catalytically-aided combustion oxidation (Model: Shimadzu TOC-L CPH/CPN, Japan). Field blank
132 filters were also analyzed using the same analytical procedure and subtracted from the respective $PM_{2.5}$ and PM_{10}

samples to obtain the analytical results (WSOC and WIOC = OC−WSOC)). Calibration of the instrument was performed before analysis of the samples using standard solution of five different concentrations. 3-10% of repeatability errors were estimated in WSOC analysis (n=3). The detail, analytical procedures is described in Rai et al. (2020a).

Wavelength Dispersive X-ray Fluorescence Spectrometer (WD-XRF) was used to analyzed the concentrations of Al, Fe, Ti, Cu, Zn, Mn, Cr, Ni, Mo, Cl, P, S, K, Zr, Pb, Na, Mg, Ca, and B in $PM_{2.5}$ and PM_{10} (with repeatability errors 5-10%). The samples were analyzed in triplicate and for major and trace elements. The detail, analytical procedures is available in Jain et al. (2020a;b).

2.3 Primary organic carbon (POC) and secondary organic carbon (SOC)

The concentrations of POC in $PM_{2.5}$ and PM_{10} samples are estimated using minimum OC/EC ratio for the each season (winter, summer, monsoon and post-monsoon). Both OC and EC in ambient aerosols are considered to be originated from combustion sources and EC is a good marker for POC (Castro et al. 1999). POC are computed using the following equation,

$$POC = [OC/EC]_{min} \times [EC] + c \quad (1)$$

where, c is the contribution from non-combustion sources which is negligible in the present case. SOC is estimated as the difference of OC and POC (SOC= OC–POC).

2.4 Enrichment Factors (EFs)

Crustal EFs referes the origin of the elements (either anthropogenic or natural) and their abundance in the ambient particulates (Amato et al., 2016). The EFs of the elements present in $PM_{2.5}$ and PM_{10} samples are computed (Taylor and McLennan, 1995) as:

$$EF = \frac{El_{sample}/X_{sample}}{El_{crust}/X_{sample}} \quad (2)$$

where,

El_{sample} = element (El) mass concentration

X_{sample} = reference element (X) mass concentration

El_{crust} = element (El) concentration in upper continental crust

X_{crust} = reference element (X) concentration in upper continental crust

Aluminium (Al) is used as the reference element in this study, which is also supported by the previous studies (Sharma et al. 2014a; 2020b).

2.5 Principal component analysis (PCA)

In this study, PCA was applied on chemical constituents of $PM_{2.5}$ and PM_{10} to identify the potential sources contributing to fine and coarse fractions aerosols. It uses orthogonal decomposition to identify individual groups of components which are then tied to variables by loading factors (Viana et al. 2008). The total variability of the data sets is shared between these components, whereas the maximum is shared by the first component (Belize et al. 2013). In PCA, the chemical data are transformed into a dimensionless standardized form:

$$Zij = \frac{Cij - \overline{Cj}}{\sigma j} \quad (2)$$

where i = 1, …, n samples; j=1, …m elements; Cij is the concentration of element j in sample i; and $\overline{Cj}$ and σj are the arithmetic mean concentration and the standard deviation for element j, respectively. The PCA model is expressed as:

$$Z_{ij} = \sum_{k=1}^{p} g_{ik} h_{kj} \quad (3)$$

Where k = 1, …, p sources, and g_{ik} and h_{kj} are the factor loadings and the factor scores, respectively. This equation is solved by Eigenvector decomposition (Song et al. 2006).

3. Results and discussion

3.1. Seasonal variations of chemical species of $PM_{2.5}$ and PM_{10}

3.1.1. Seasonal variability of $PM_{2.5}$ and PM_{10}

The annual average $PM_{2.5}$ and PM_{10} concentrations were estimated as 37±12 μg m^{-3} (range: 16−77 μg m^{-3}) and 56±18 μg m^{-3} (range: 21−116 μg m^{-3}), respectively (Table 1). The maximum monthly average mass concentration of $PM_{2.5}$ was recorded in October (58 μg m^{-3}) and the minimum monthly average concentration of $PM_{2.5}$ was observed in January (27 μg m^{-3}). Whereas, monthly average maxima of PM_{10} was observed in March (73 μg m^{-3}) and monthly average minima in the month of January (43 μg m^{-3}). The monthly average and temporal variations in $PM_{2.5}$ and PM_{10} concentrations are shown in Figs.S2-S3 (see the supplementary information). The highest seasonal average concentration of both $PM_{2.5}$ (41±14 μg m^{-3}) and PM_{10} (64±20 μg m^{-3}) were found during summer and minimum seasonal average mass concentration of both $PM_{2.5}$ (31±9 μg m^{-3}) and PM_{10} (51±17 μg m^{-3}) were recorded during

189 winter. In post-monsoon, the mass concentrations of $PM_{2.5}$ (40±11 µg m^{-3}) and PM_{10} (55±17 µg m^{-3}) were recorded
190 higher than the winter and monsoon (Table 1). In the present case, non-significant seasonal variation in mass
191 concentrations of both $PM_{2.5}$ and PM_{10} was recorded at Darjeeling (except winter). Sharma et al. (2014b) reported
192 the similar concentration of $PM_{2.5}$ (at Kullu: 34±2 µg m^{-3}; at Shimla: 32±3 µg m^{-3}) at the north-western Himalayan
193 region during winter 2013, whereas Kaushal et al. (2018) recorded the 52±18 µg m^{-3} of PM_{10} concentration at
194 Pohara of north-western Himalaya (Himachal Pradesh) during winter 2015. Sharma et al. (2020a) reported the PM_{10}
195 concentration as 54±12 µg m^{-3} and 39±10 µg m^{-3} during post-monsoon and winter, respectively at Nainital a central
196 Himalaya. Sharma et al. (2020b) also reported the PM_{10} concentration as 48±16 µg m^{-3} during winter in Darjeeling.
197 The monthly variation in mass concentration of $PM_{2.5}$ and PM_{10} in relation ambient temperature, RH, wind direction
198 and wind speed is depicted in Figs.S1-S2 (see the supplementary information). It has been observed that the
199 prevailing meteorology of the sampling site influenced the seasonal variation in mass concentrations of $PM_{2.5}$ and
200 PM_{10} at Darjeeling. However, the higher concentration of pollutants during the summer season at Darjeeling might
201 be due to more influence of tourism activities (Gajananda et al. 2005; Chatterjee et al. 2021) as well as long-range
202 transportation of pollutants at sampling site of the Darjeeling (Rai et al. 2020a).
203
204 **3.1.2. Variation of OC, EC and WSOC in $PM_{2.5}$ and PM_{10}**
205 Temporal variations in OC, EC and WSOC concentrations of $PM_{2.5}$ and PM_{10} during study period are shown in
206 Fig.S3 (b-d) (see the supplementary information). The annual average concentrations of OC, EC, WSOC and WIOC
207 of $PM_{2.5}$ were 3.46±1.59 µg m^{-3}, 1.93±0.93 µg m^{-3}, 1.88±1.05 µg m^{-3} and 1.69±0.85 µg m^{-3}, respectively. Whereas
208 the annual average of OC, EC, WSOC and WIOC in PM_{10} were 5.06±2.03 µg m^{-3}, 2.34±1.18 µg m^{-3}, 3.55±1.75 µg
209 m^{-3} and 1.51±0.92 µg m^{-3}, respectively. Figure 2 shows the monthly average of OC, EC and WSOC in $PM_{2.5}$ and
210 PM_{10} during study period in Darjeeling. Highest monthly average OC in $PM_{2.5}$ (4.76 µg m^{-3}) and PM_{10} (6.30 µg m^{-3})
211 was found in November (post-monsoon), whereas monthly average minima of OC in $PM_{2.5}$ (2.03 µg m^{-3}) and PM_{10}
212 (3.31 µg m^{-3}) was found in August (monsoon) and May (summer), respectively. Similar monthly average maxima
213 and minima of EC (in $PM_{2.5}$ and PM_{10}) was recorded in March and August, respectively (Fig. 2). Highest monthly
214 average WSOC concentration in both $PM_{2.5}$ (2.77 µg m^{-3}) and PM_{10} (5.51 µg m^{-3}) was recorded in November (post-
215 monsoon) might be due to the influence of stubble burning in northern states of India (Punjab, Haryana and western
216 Utter Pradesh of IGP). Figure 3 shows the seasonal average OC, EC, WSOC, WIOC, POC, SOC and TCA

concentrations of $PM_{2.5}$ and PM_{10} during winter, summer, monsoon and post-monsoon seasons in Darjeeling. Highest seasonal average OC concentration of $PM_{2.5}$ (4.07±1.55 µg m^{-3}) and PM_{10} (5.69±2.09 µg m^{-3}) was recorded in post-monsoon season and minimum seasonal average concentration of OC in $PM_{2.5}$ (2.21±0.86 µg m^{-3}) and PM_{10} (3.62±0.86 µg m^{-3}) was recorded during monsoon (Table 1). Similarly, seasonal average maxima and minima of EC in $PM_{2.5}$ and PM_{10} were recorded in summer and monsoon seasons, respectively. Average WSOC in both $PM_{2.5}$ (2.17±0.98 µg m^{-3}) and PM_{10} (4.44±1.55 µg m^{-3}) were found highest during post-monsoon season and minimum in monsoon season (Fig. 3).

The annual average concentration of TCA contributes 20.6% of $PM_{2.5}$ (7.6±3.4 µg m^{-3}) and 18.6% of PM_{10} (10.4±4.3 µg m^{-3}). The highest TCA in $PM_{2.5}$ and PM_{10} were recorded in winter (22.7% of $PM_{2.5}$ and 22.4% of PM_{10}) season followed by post-monsoon (21.7% of $PM_{2.5}$ and 20.3% of PM_{10}), summer (21.6% of $PM_{2.5}$ and 17.6% of PM_{10}) and monsoon (12.5% of $PM_{2.5}$ and 13.4% of PM_{10}) seasons. The annual average concentration of POC in $PM_{2.5}$ was recorded to be 2.35 ± 1.06 µg m^{-3} (66% of OC), and SOC was 1.19±0.57 µg m^{-3} (34% of OC). Similarly, the annual average POC concentration in PM_{10} was recorded as 3.18 ± 1.13 µg m^{-3} (63% of OC), whereas, SOC was recorded as 2.05±0.98 µg m^{-3} (37% of OC). In $PM_{2.5}$ the seasonal contribution of POC and SOC were ranging from 55-77% and 33-45% of OC, respectively, whereas in PM_{10} the seasonal contribution of POC and SOC were ranging from 51-73% and 37-49% of OC, respectively. Sen et al. (2018) reported the similar OC (7.7±0.7 µg m^{-3}) and EC (3.7±0.6 µg m^{-3}) concentrations in PM_{10} at Darjeeling and high OC (10.3±5.6 µg m^{-3}) and EC (5.4±2.9 µg m^{-3}) values in PM_{10} at Kullu-Mohal (north-western Himalayas) during winter. Whereas, Rai et al. (2020a) observed the low OC (3.7±1.3 µg m^{-3}) and EC (1.3±0.6 µg m^{-3}) in PM_{10} at Darjeeling. Sharma et al. (2020a) also found the similar OC and EC concentrations in PM_{10} over Nainital (central Himalayas) during post-monsoon (OC: 4.7±1.1 µg m^{-3} and EC: 1.1±0.5 µg m^{-3}) and winter (OC: 3.2±1.1 µg m^{-3} and EC: 1.4±0.6 µg m^{-3}) seasons.

Figure 2 shows the monthly average OC/EC and WSOC/OC ratios of $PM_{2.5}$ and PM_{10} at Darjeeling, whereas seasonal relationship between OC and EC, WSOC and OC of $PM_{2.5}$ and PM_{10} are depicted in Figs. S4-S5 (see the supplementary information). The seasonal average OC/EC of $PM_{2.5}$ was 1.87 (range: 1.40 - 2.81), 1.92 (range: 1.22 - 2.82), 1.85 (range: 1.30 - 2.57) and 1.94 (range: 1.05 -2.87) during winter, summer, monsoon and post-monsoon, respectively. The seasonal average WSOC/OC ratio of $PM_{2.5}$ was computed as 0.50, 0.52, 0.53 and 0.54 during winter, summer, monsoon and post-monsoon, respectively. Similarly, the seasonal average OC/EC of PM_{10} was 2.04, 1.74, 3.37 and 3.01 during winter, summer, monsoon and post-monsoon, respectively, whereas, the seasonal

245 average WSOC/OC of PM_{10} was 0.71, 0.61, 0.65 and 0.79 during winter, summer, monsoon and post-monsoon,
246 respectively. Hegde et al. (2016) also observed a similar (0.51±0.06 for TSP) WSOC/OC value in Nainital during
247 winter. Due to poor solubility of organics emitted from the combustion of liquid fossil fuels the WSOC/OC values
248 for vehicular emissions are low as compared to biomass burning. In this study, significant positive correlation
249 between OC *vs.* EC (for $PM_{2.5}$: R^2 = 0.88, 0.86, 0.63 and 0.80 at p <0.05; for PM_{10}: R^2 = 0.77, 0.85, 0.09 and 0.74 at
250 p <0.05 during winter, summer, monsoon and post-monsoon seasons, respectively) of $PM_{2.5}$ and PM_{10} has been
251 observed during all the seasons (except monsoon season for PM_{10}) (Figs. S4-S5; in supplementary information),
252 which is indicative of their common sources (Rengarajan et al. 2007; Ram and Sarin 2011). The scatter plots
253 between WSOC and OC (for $PM_{2.5}$: R^2 = 0.63, 0.73, 0.62 and 0.83; and for PM_{10}: R^2 = 0.69, 0.91, 0.17 and 0.87
254 during winter, summer, monsoon and post-monsoon seasons, respectively) of $PM_{2.5}$ and PM_{10} (except monsoon
255 season for PM_{10}) shows significant positive correlation suggesting that both OC and EC are obtained from the same
256 primary emission source or by similar secondary processes (Figs. S4-S5; in supplementary information). The non-
257 significant positive correlation of K (a tracer of biomass) with Ca, Mg, WSOC of $PM_{2.5}$ and significant positive
258 correlation of K with Ca, Mg, WSOC of PM_{10} during all the seasons (except post-monsoon season for $PM_{2.5}$)
259 demonstrate the abundance of soil/road dust contributed by soluble organic sources to $PM_{2.5}$ and PM_{10} at study site
260 (Tables: S1-S8; in supplementary information). I may also be considered that the soil suspension, fuel combustion
261 (Urban et al. 2012), and formation of secondary water soluble organic aerosols (Lim et al. 2010) might be the some
262 other sources of WSOC in the sampling site of Darjeeling.
263
264 **3.1.3. Major and trace elements in $PM_{2.5}$ and PM_{10}**
265 During the sampling 17 common elements (Al, Fe, Ti, Cu, Zn, Mn, Cr, Ni, Mo, Cl, P, S, K, Zr, Pb, Na, Mg, Ca,
266 and B) were extracted in $PM_{2.5}$ and PM_{10} (Cu and Pb in PM_{10} but traced in few $PM_{2.5}$ samples also) using X-RF
267 technique of sampling site (Table 1). In $PM_{2.5}$ samples, Na has observed highest annual average concentration
268 (1.014 ± 0.392 µg m^{-3}) followed by Ca (0.918 ± 0.813 µg m^{-3}), S (0.667 ± 0.404 µg m^{-3}), Fe (0.502 ± 0.195 µg m^{-3}),
269 K (0.388 ± 0.224 µg m^{-3}), and so on with higher loading in summer season (Table 1). Whereas in case of PM_{10}, S
270 has recorded highest annual average concentration (1.260 ± 0.744 µg m^{-3}) followed by Ca (0.985 ± 0.299 µg m^{-3}),
271 Al (0.922 ± 0.446 µg m^{-3}), K (0.650 ± 0.376 µg m^{-3}), Fe (0.635 ± 0.266 µg m^{-3}), Na (0.607 ± 0.396 µg m^{-3}), and so
272 on. The annual average concentrations of elements in $PM_{2.5}$ and PM_{10} are 5.71 ± 3.67 µg m^{-3} (accounted for 15% of

273 $PM_{2.5}$) and 6.44 ± 3.58 µg m^{-3} (accounted for 12% of PM_{10}), respectively. The monthly average concentrations of
274 elements of $PM_{2.5}$ and PM_{10} are shown in Fig. S6 (see the supplementary information). Higher average
275 concentrations of elements are recorded during summer (21% of $PM_{2.5}$ and 12% of PM_{10}) followed by winter
276 (16.5% of $PM_{2.5}$ and 11.7 of PM_{10}), post-monsoon (11.6% of $PM_{2.5}$ and 11% of PM_{10}) and monsoon (9% of $PM_{2.5}$
277 and 13% of PM_{10}) seasons (Fig. 4). During winter 2013 land campaign, Sharma et al. (2014b) found the Na, Mg, Ca,
278 Al, P, S, Si, Cl, K, Ti, Sr, Zr, Pb, Sb, Ag, Cs, Hg, Mn, Fe and Zn in $PM_{2.5}$ (which had accounted for ~27% of $PM_{2.5}$)
279 over the north-western Himalaya. Sharma et al. (2020a) also reported the elements contribution to PM_{10} as 16% and
280 13% during post-monsoon and winter seasons, respectively at central Himalaya (Nainital). The similar contribution
281 of elements to the PM_{10} over the Himalayan region and other high altitude regions are discussed in our earlier
282 publication (Sharma et al. 2020b).

283 Figure 5 represents the seasonal enrichment factors (EFs) of the elements (Al, Fe, Ti, Cu, Zn, Mn, Cr, Ni, Mo,
284 Cl, P, S, K, Zr, Pb, Na, Mg, Ca, and B) available in $PM_{2.5}$ and PM_{10} samples. Al, Fe, Ti, K, Mg, and Ca in both
285 $PM_{2.5}$ and PM_{10} have recorded low EFs (< 5) for all the seasons, which indicate that, elements mostly arrived from
286 crustal/soil sources. The element like Cu, Zn, Ni, Pb, Cr, Mo and B have higher EFs (>10) in both $PM_{2.5}$ and PM_{10}
287 and therefore are likely of anthropogenic origin. The higher the EF of Cr, Ni, Pb and Zn of PM were also attributed
288 to industrial emission (IE) sources. Generally Cu, Mn, Zn, Ni, Cd, Fe, Mo, S and Cr use as a marker for IE in India
289 (Shridhar et al. 2010).

290 The annual and seasonal statistical summary of elements recorded in $PM_{2.5}$ and PM_{10} samples is tabulated in
291 Table 1. The possible sources of trace metals present in a fine and coarse fraction of particulates can be primarily
292 crustal/mineral dust. In this study, Al, is significantly positive correlated with Fe, Ca, Mg and Ti (as well as with
293 PM_{10}) and the average Fe/Al ratio is 0.69 (winter: 0.76; summer: 0.74; monsoon: 0.45 and post-monsoon: 0.79),
294 which indicates the dominant source of mineral dust. Similarly, Ca/Al ratio (1.07) indicates that PM over the eastern
295 Himalayan region is rich in Ca mineral as compared to average continental crust. Similar results were also observed
296 in case of elements extracted in $PM_{2.5}$ over the eastern Himalaya. Sarin et al. (1979) had reported that the Fe/Al ratio
297 in north Indian plains ranged from 0.55 to 0.63. Kumar and Sarin (2009) reported Fe/Al ratio as 0.59 for $PM_{2.5-10}$ at
298 a remote high altitude sampling site (Manora Peak) of western India. McLennan, (2001) recorded the average Ca/Al
299 ratio as 1.07 in PM_{10} whereas, the corresponding ratio in the upper continental crust is 0.38. Sharma et al. (2020a)
300 also reported Ca/Al ratio as 1.52 and 1.19 in PM_{10} during post-monsoon and winter seasons, respectively at central

Himalayas (Nainital), whereas Kumar and Sarin (2009) had recorded the Ca/Al ratio as 0.73 in $PM_{2.5}$ and 1.74 in PM_{10} at Manora Peak, a high altitude site of the western India. The significant positive correlation of Al with Fe, Ca, Mg and Ti of coarse and fine (except few in $PM_{2.5}$) fractions of PM during all the seasons are also indicated the abundance of mineral dust at the sampling site of Darjeeling (Table S1-S8; in supplementary information).

3.2. Possible sources and source regions

3.2.1 Possible sources of $PM_{2.5}$ and PM_{10}

PCA has been performed with chemical species of $20PM_{2.5}$ and $22PM_{10}$ (OC, EC, WSOC, Na, Ca, Mg, Al, Fe, Ti, K, Cl, P, S, Cr, Ni, Cu, Zn, Mn, Mo, Zr, Pb and B) to identify the factor loading to $PM_{2.5}$ and PM_{10}. The factor profiles (a yearlong data) of the possible sources of $PM_{2.5}$ and PM_{10} extracted by PCA are summarized in Table 2. On the basis of the factor loading PCA resolved the four common sources [biomass burning + fossil fuel combustion (BB+FFC), crustal/soil dust (SD), vehicular emissions (VE) and industrial emissions (IE)] of $PM_{2.5}$ and PM_{10} at Darjeeling.

Factor 1: The first factor of $PM_{2.5}$ represents the BB+FFC, characterized (38.3% of the variance) by highly loaded with OC, EC, WSOC, K, Cl and S. K^+ and Levoglucoson are considered BB (cow dung, crop residue, fuel wood, and wildfires, etc.) marker, whereas presence of Cl in the factor reveals the wood and coal burning (Pant and Harrison, 2012). WSOC/OC and OC/EC mass ratios also evidence the BB+FFC as a one of the sources of $PM_{2.5}$ at the observational site of Darjeeling (Sharma et al. 2020b; Chatterjee et al. 2021). The first factor of PM_{10} represented by high loading (36.7% of the variance) of crustal elements like, Al, Ti, Fe, Ca, Mg, K and Na which inferred the source as crustal/soil/road dust (Begam et al. 2011; Sharma et al. 2014a; Jain et al. 2020b). The abundance of these elements at the study site as crustal origin is also confirmed by EFs (Fig. 5) as well as positive correlations of Al with Ca, Mg and Ti (Table S1-S8).

Factor 2: This factor of $PM_{2.5}$ was resolved as crustal/soil dust by high loading of Al, Ti, Fe, Ca, Mg, K and Na (17.6% of the variance of factor loading) (Table 2). The EFs of these elements are also suggesting the crustal origin the elements at sampling site (Fig. 5) as well as the positive correlations of Al with Ca, Mg and Ti. Whereas second factor of PM_{10} represented by BB+FFC with high loadings of OC, EC, WSOC, K, Cl and S (Begam et al. 2011; Pant and Harrison 2012). WSOC/OC and OC/EC ratios are also suggesting the influence of BB+FFC as a source of PM_{10} at Darjeeling (Sharma et al. 2020b; Chatterjee et al. 2021).

Factor 3: The third factor of both $PM_{2.5}$ and PM_{10} constitutes the vehicular emissions (VE) with the dominant presence of EC, OC, Zn, Mn, Zr and B, indicates the emission derived from road side vehicles (Pant and Harrison, 2012; Jain et al. 2020b). Since, EC and OC are majorily emitted from the combustion sources, so these components are considered as important tracers for VE globally (Yin et al. 2010; Begam et al. 2011). Zn and Mn are used as marker of brake and tire wear, two stroke engine emissions (Zn as fuel additive), heavy duty diesel truck emission (Mn as fuel additive) (Kothai et al. 2008; Sharma et al. 2014a). VE is inferred to be one of the major sources of aerosols (Sharma et al. 2020b) at in urban sites of Himalayan region may due to the great influence of tourism activities (Gajananda et al. 2005; Chatterjee et al. 2021).

Factor 4: The fourth source of both $PM_{2.5}$ and PM_{10} is characterized as industrial emissions (IE) considering to the higher loading of Cu, Zn, Ni, Cr and Mo in aerosol samples (Table 2). These metals (Cu, Zn, Ni, Cr and Mo) might be originated from the small to medial scale industries, metal processing industries and industrial effluents (Gupta et al. 2007; Jain et al. 2019). Sharma et al. (2020b) also reported the solid waste + IE a source of PM_{10} in Darjeeling with these marker elements.

3.2.2 Air mass backward trajectory

To investigate the transport pathway of fine ($PM_{2.5}$) and coarse fractions (PM_{10}) of aerosols at the observational site of Darjeeling, 5-days air-mass back trajectory was computed using the HYSPLIT model (Draxeler and Ralph. 2003) at an altitude of 100m, 500 m and 100m AGL for all the sampling day (Fig.6). In the present case, air parcels approaching to sampling site of Darjeeling is mainly from Bhutan, Nepal, China, Arunachal Pradesh, IGP (Punjab, Haryana, Uttar Pradesh, Bihar and West Bengal) and surrounding regions during all the seasons. During monsoon season, air mass also approaching to sampling site from Bay of Bengal. Chatterjee et al. (2021) reported the similar air parcels towards the Darjeeling during summer and winter season (Sharma et al. 2020b).

4. Conclusions

In this study seasonal variation in carbonaceous aerosols and elements in fine and coarse fractions of aerosol ($PM_{2.5}$ and PM_{10}) were estimated to explore the prominent sources of $PM_{2.5}$ and PM_{10} in the high altitude of eastern Himalaya during August 2018 - July 2019. The average $PM_{2.5}$ and PM_{10} concentrations were recorded as 37±12 µg m^{-3} and 58±18 µg m^{-3}, respectively during the study. The annual total carbonaceous aerosols in $PM_{2.5}$ and PM_{10} were

accounted for 20.6% of $PM_{2.5}$ and 18.6% of PM_{10}, respectively (along with season variation). The concentrations of elements present in $PM_{2.5}$ and PM_{10} were accounted for 15% and 12%, respectively. During all the seasons, significant positive linear relationship between OC and EC; and OC and WSOC (as well as OC/EC and WSOC/OC) indicate the common sources (BB+FFC) of both $PM_{2.5}$ and PM_{10}. EFs analysis the elements present in PM indicates the abundance of mineral dust at the eastern Himalaya. PCA resolved the four common sources [(BB+FFC), crustal/SD, (VE) and (IE)] of $PM_{2.5}$ and PM_{10} at Darjeeling. 5 days HYSPLIT back trajectory air parcels indicate that the pollutants approaching to Darjeeling are mainly from Bhutan, Nepal, China, Arunachal Pradesh and IGP region (Punjab, Haryana, Uttar Pradesh, Bihar and West Bengal) during all the seasons as well as the Bay of Bengal (mainly in monsoon season).

Acknowledgement:

The authors are thankful to the Director, CSIR-NPL and Head, Environmental Sciences and Biomedical Division (ES&BMD), CSIR-NPL for their encouragement and support. Authors are also thankful to Mr. Bivek Gurung and Mrs. Yashodhara Yadav, Bose Institute, Darjeeling for PM sampling and providing the relevant data-sets. Authors thankfully acknowledge the NOAA Air Resources Laboratory for download the air mass trajectories (http://www.arl.noaa.gov/ready/hysplit4.html).

Funding:

The authors are thankfully acknowledged the Department of Science and Technology, Ministry of Science and Technology (Government of India), New Delhi-110016, India for providing financial support for this study (DST/CCP/Aerosol/88/2017).

Authors' contributions: Conception and design of the study were planned by SKS; Data collection and analysis were performed by NV, NC, AR, DS, SM and AG; the first draft was written by SKS. Data interpretation was carried out by SKS, AC, TKM and NV. All the authors read and approved the final manuscript.

Data availability: The datasets developed during the current study are available from the corresponding author on reasonable request.

385

386 **Compliance with ethical standards**

387 **Competing interests**: The authors declare that they have no conflict of interest.

388 **Ethical approval**: Not applicable.

389 **Consent to participate**: Not applicable.

390 **Consent to publish**: Not applicable.

391

392 **References**

393 Adak A, Chatterjee A, Singh A K, Sarkar C, Ghosh S, Raha S (2014) Atmospheric fine mode particulates at eastern
394 Himalaya, India: role of meteorology, long-range transport, and local anthropogenic sources. Aerosol Air
395 Qual Res 14(1): 440-450

396 Amato F, Alastuey A, Karanasiou A, Lucarelli F, Nava S, Calzolai G, Severi M, Becagli S, Vorne LG, Colombi C,
397 Alves C, Custódio D, Nunes T, Cerqueira M, Pio C, Eleftheriadis K, Diapouli E, Reche C, Minguillón MC,
398 Manousakas MI, Maggos T, Vratolis S, Harrison RM, Querol X (2016) IRUSE-LIFE. Atmos Chem Phys
399 16:3289-309

400 Begam G R, Vachaspati CV, AhammedYN, Kumar KR, Reddy RR, Sharma SK, Saxena M, Mandal TK (2017)
401 Seasonal characteristics of water soluble inorganic ions and carbonaceous aerosols in total suspended
402 particulate matter at a rural semi-arid site, Kadapa (India). Environ Sci Poll Res 24(2): 1719-1734

403 Begum B A, Hossain A, Saroar G, Biswas S K, Nasiruddin M, Nahar N, Chowdury Z, Hopke P K (2011) Sources of
404 carbonaceous materials in the airborne particulate matter of Dhaka. Asian J Atmos Environ 5(4): 237–246

405 Behera SN, Sharma M (2010) Investigating the potential role of ammonia in ion chemistry of fine particulate matter
406 formation for an urban environment. Sci Total Environ 408(17): 3569–3575

407 Belis C, Karagulian F, Larsen B, Hopke P (2013) Critical review and meta-analysis of ambient particulate matter
408 source apportionment using receptor models in Europe. Atmos Environ 69: 94-108

409 Bond TC, Doherty SJ, Fahey DW, Forster PM, Berntsen T, DeAngelo BJ, Flanner MG, Ghan S, Kärcher B, Koch D,
410 Kinne S (2013) Bounding the role of black carbon in the climate system: A scientific assessment. J Geophy
411 Res 118(11):5380-552

412 Cao J, Lee S, Ho K, Fung K, Chow JC, Watson JG (2006) Characterization of roadside fine particulate carbon and
413 its eight fractions in Hong Kong. Aerosol Air Qual Res 6 (2): 106-122
414 Castro LM, Pio CA, Harrison RM, Smith DJT (1999) Carbonaceous aerosol in urban and rural European
415 atmospheres: estimation of secondary organic carbon concentrations. Atmos Environ 33: 2771–2781
416 Chatterjee A, Adak A, Singh, A K, Srivastava M K, Ghosh S K, Tiwari S, Devara PCS, Raha S (2010) Aerosol
417 chemistry over a high-altitude station at the north-eastern Himalayas, India. PloS one 5(6):11122
418 Chatterjee A, Mukherjee S, Dutta M, Ghosh A, Ghosh SK, Roy A (2021) High rise in carbonaceous aerosols under
419 very low anthropogenic emissions over eastern Himalaya, India: Impact of lockdown for COVID-19
420 outbreak. Atmos Environ 244:117947.
421 Chow J C, Watson JG, Chen L W A, Arnott W P, Moosmuller H (2004) Equivalence of elemental carbon by
422 thermal/optical reflectance and transmittance with different temperature protocols. Environ Sci Technol 38:
423 4414–4422
424 Draxler RR, Rolph GD (2003) HYSPLIT (HYbrid Single-particle Lagrangian Integrated Trajectory) Model. Access
425 via NOAA ARL READY website. NOAA Air Resources Laboratory, Silver Spring.
426 http://www.arl.noaa.gov/ready/hysplit4.html
427 Gajananda K, Kuniyal JC, Momin GA, Rao PSP, Safai PD, Tiwari S, Ali K (2005) Trend of atmospheric aerosols
428 over the north northwestern Himalayan region, India. Atmos Environ 39: 4817-4825
429 Gupta AK, Karar K, Srivastava A (2007) Chemical mass balance source apportionment of PM_{10} and TSP in
430 residential and industrial sites of an urban region of Kolkata, India. J Hazardous Materials 142:279-287
431 Gupta S, Gadi R, Sharma SK, Mandal TK (2018) Characterization and source apportionment of organic compounds
432 in PM_{10} using PCA and PMF at a traffic hotspot of Delhi. Sustain Cities Soc 39: 52–67
433 Hansen J M, Sato R, Rued L, Nazarenko A, Lacis GA, Schmidt G, Russell I, Aleinov M, Bauer S, Bauer N, Bell B,
434 Cairns V, Canuto M, Chandler Y, Cheng A, Del Genio G, Faluvegi E, Fleming A, Friend T, Hall C,
435 Jackman M, Kelley NY, Kiang D, Koch J, Lean J, Lerner K, Lo S, Menon RL, Miller P, Minnis T,
436 Novakov V, Oinas JP, Perlwitz J, Perlwitz D, Rind A, Romanou D, Shindell P, Stone S, Sun N,
437 Tausnev D, Thresher B, Wielicki T, Wong M Y, Zhang X (2005) Efficacy of climate forcings. J Geophys
438 Res 110, D18104

439 Hegde P, Kawamura K, Joshi H, Naja M (2016) Organic and inorganic components of aerosols over the central
440 Himalayas: winter and summer variations in stable carbon and nitrogen isotopic composition. Environ Sci
441 Poll Res 23:6102-6118
442 Jacobson MZ (2002) Control of fossil fuel particulate black carbon and organic matter, possibly the most effective
443 method of slowing global warming. J Geophys Res 107(19): 4410
444 Jain S, Sharma S K, Vijayan N, Mandal TK (2020) Seasonal characteristics of aerosols ($PM_{2.5}$ and PM_{10}) and their
445 source apportionment using PMF: A four year study over Delhi, India. Environ Poll 262: 114337
446 Jain S, Sharma SK, Choudhary N, Masiwal R, Saxena M, Sharma A, Mandal TK, Gupta A, Gupta NC, Sharma C
447 (2017) Chemical characteristics and source apportionment of $PM_{2.5}$ using PCA/APCS, UNMIX, and PMF
448 at an urban site of Delhi, India. Environ Sci Poll Res 24(17):14637-14656
449 Jain S, Sharma SK, Vijayan N, Mandal TK (2020a) Investigating the seasonal variability in source contribution to
450 $PM_{2.5}$ and PM_{10} using different receptor models during 2013–2016 in Delhi, India. Environ Sci Poll Res
451 https://doi.org/10.1007/s11356-020-10645-y
452 Kanakidou M, Seinfeld JH, Pandis SN, Barnes I, Dentener FJ, Facchini MC, Dingenen RV, Ervens B, Nenes
453 ANCJSE, Nielsen CJ, Swietlicki E (2005) Organic aerosol and global climate modelling: a review. Atmos
454 Chem Phy 5(4):1053-1123
455 Kaushal D, Kumar A, Yadav S, Tandon A, Attri AK (2018) Wintertime carbonaceous aerosols over Dhauladhar
456 region of North-Western Himalayas. Environ Sci Poll Res 25:8044–8056
457 Kothai P, Saradhi IV, Prathibha P, Hopke PK, Pandit GG, Puranik VD (2008) Source apportionment of coarse and
458 fine particulate matter at Navi Mumbai,India. Aerosol Air Qual Res 8(4): 423–436
459 Kumar A, Attri A K (2016) Biomass combustion a dominant source of carbonaceous aerosols in the ambient
460 environment of western Himalayas. Aerosol Air Qual Res 16(3): 519–529
461 Kumar A, Sarin MM (2009) Mineral aerosols from western India: temporal variability of course and fine
462 atmospheric dust and elemental characteristics. Atmos Environ 43:4005-4013
463 Lighty J S, Veranth JM, Sarofim AF (2000) Combustion aerosols: factors governing their size and composition
464 implications to human health. J Air Waste Manag Assoc 50 (9):1565-1618
465 Lim HJ, Turpin B J (2002) Origins of primary and secondary organic aerosol in Atlanta: Results of time-resolved
466 measurements during the Atlanta supersite experiment. Environ Sci Technol 36: 4489-4496

467 Lim Y B, Tan Y, Perri M J, Seitzinger S P, Turpin B J (2010) Aqueous chemistry and its role in secondary organic
468 aerosol (SOA) formation. Atmos Chem Phys Discussions 10(6)
469 Mandal P, Sarkar R, Mandal A, Saud T (2014). Seasonal variation and sources of aerosol pollution in Delhi, India.
470 Environ Chem Lett 12(4): 529–534
471 McLennan S (2001) Relationship between the trace element composition of sedimentary rocks and upper continental
472 crust. Geochem Geophys Geosyst 2:1021, doi: 10.1029/ 2000/ GC 000109
473 Morawska L, Zhang JJ (2002) Combustion sources of particles. Health relevance and source
474 signatures. Chemosphere 49: 1045–1058
475 Pant P, Harrison R M (2012) Critical review of receptor modeling for particulate matter: a case study of India.
476 Atmos Environ 49: 1–12
477 Pope C A, Ezzati M, Dockery DW (2009) Fine-particulate air pollution and life expectancy in the United
478 States. New England Journal of Medicine 360(4): 376-386
479 Rai A, Mukherjee S, Chatterjee A, Choudhary N, Kotnala G, Mandal TK, Sharma SK (2020a) Seasonal variation of
480 OC, EC and WSOC of PM10 and their CWT analysis over the eastern Himalaya. Aerosol Sci Eng 4:26-40
481 Rai P, Furger M, El Haddad I, Kumar V, Wang L, Singh A, Dixit K, Bhattu D, Petit JE, Ganguly D, Rastogi N
482 (2020b) Real-time measurement and source apportionment of elements in Delhi's atmosphere. Sci Total
483 Environ 742:140332
484 Ram K, Sarin M, Hegde P (2008) Atmospheric abundances of primary and secondary carbonaceous species at two
485 high altitude sites in India: sources and temporal variability. Atmos Environ 42(28): 6785-6796
486 Ram K, Sarin MM (2011) Day–night variability of EC, OC, WSOC and inorganic ions in urban environment of
487 Indo-Gangetic Plain: Implications to secondary aerosol formation. Atmos Environ 45:460-468
488 Ramana MV, Ramanathan V, Feng Y, Yoon SC, Kim SW, Carmichael G R, Schauer J J (2010) Warming influenced
489 by the ratio of black carbon to sulphate and the black-carbon source. Nat Geosci 3:542–545
490 Ramgolam K, Favez O, Cachier H, Gaudichet A, Marano F, Martinon L (2009) Size-partitioning of an urban aerosol
491 to identify particle determinants involved in the pro-inflammatory response induced in airway epithelial
492 cells. Particle and Fibre Toxicology 6(1), doi:10.1186/1743-8977-6-10
493 Rastogi N, Sarin M M (2009) Quantitative chemical composition and characteristics of aerosols over western India:
494 One-year record of temporal variability. Atmos Environ 43(22-23): 3481-3488

Rengarajan R, Sarin MM, Sudheer AK (2007) Carbonaceous and inorganic species in atmospheric aerosols during wintertime over urban and high-altitude sites in North India. J Geophy Res 112:D21307

Robinson A L, Donahue N M, Shrivastava M K, Weitkamp E A, Sage A M, Grieshop A P, Pandis S N, (2007) Rethinking organic aerosols: Semivolatile emissions and photochemical aging. Science 315 (5816):1259-1262

Sarin MM, Borole DV, Krishnaswami S (1979) Geochemistry and geochronology of sediments from the Bay of Bengal and the equatorial Indian Ocean. Proc. Indian Academy of Science 88:131-154

Sarkar C, Chatterjee A, Majumdar D, Roy A, Srivastava A, Ghosh S K, Raha S (2017) How the atmosphere over eastern Himalaya, India is polluted with carbonyl compounds? Temporal variability and identification of sources. Aerosol Air Qual Res 17:2206-2223

Sen A, Karapurkar S G, Saxena M, Shenoy D M, Chaterjee A, Choudhuri A K, Das T, Khan A H, Kuniyal J C, Pal S, Singh D P, Sharma S K, Kotnala R K, Mandal T K (2018) Stable carbon and nitrogen isotopic composition of PM_{10} over Indo-Gangetic Plains (IGP), adjoining regions, and Indo-Himalayan Range (IHR) during the winter 2014 campaign. Environ Sci Poll Res 25(26): 26279-26296

Sharma S K, Mandal T K, Dey A K, Deb N, Jain S, Saxena M, Pal S, Choudhuri AK, Yadav S (2018a) Carbonaceous and inorganic species in PM_{10} during wintertime over Giridih, Jharkhand (India). J Atmos Chem 75:219-233

Sharma S K, Mandal T K, Jain S, Saraswati, Sharma A, Saxena M (2016) Source apportionment of $PM_{2.5}$ in Delhi, India using PMF model. Environ Contam Toxicol 97: 286-293

Sharma S K, Mandal T K, Saxena M, Sharma A, Gautam R (2014a) Source apportionment of PM_{10} by using positive matrix factorization at an urban site of Delhi, India. Urban climate 10: 656-670

Sharma S K, Mandal T K, Sharma C, Kuniyal J C, Joshi R, Dhyani P P, Rohtash, Ghayas H, Gupta NC, Sharma P, Saxena M, Sharma A, Arya BC, Kumar A (2014b) Measurements of particulate ($PM_{2.5}$), BC and trace gases over the Northwestern Himalayan region of India. Mapan 29(4): 243–253

Sharma S K, Mandal TK, Sharma A, Saraswati, Jain S (2018b) Seasonal and annual trends of carbonaceous species of PM_{10} over a megacity Delhi, India during 2010-2017. J Atmos Chem 75: 305-318

Sharma SK, Choudhary N, Kotnala G, Das D, Mukherjee S, Ghosh A, Vijayan N, Rai A, Chatterjee A, Mandal TK (2020b) Wintertime carbonaceous species and trace metals in PM_{10} in Darjeeling: a high altitude town in the eastern Himalayas. Urban Climate 34 (4): 100668

Sharma SK, Choudhary N, Srivastava P, Naja M, Vijayan N, Kotnala G, Mandal TK (2020a) Variation of carbonaceous species and trace elements in PM_{10} at a mountain site in the central Himalayan region of India. J Atmos Chem 77(3): 49-62

Shivani, Gadi R, Sharma S K, Mandal TK (2019) Seasonal variation, source apportionment and source attributed health risk of fine carbonaceous aerosols over National Capital Region, India. Chemosphere. 237:124500

Shridhar V, Khillare P, Agarwal T, Ray S (2010) Metallic species in ambient particulate matter at rural and urban location of Delhi. J Hazard Mater 175: 600–607

Song Y, Zhang Y, Xie S, Zeng L, Zheng M, Salmon LG, Shao M, Slanina S (2006) Source apportionment of $PM_{2.5}$ in Beijing by positive matrix factorization. Atmos Environ 40 (1): 526–1537

Srinivas B, Sarin M M (2014) $PM_{2.5}$, EC, and OC in an atmospheric outflow from the Indo-Gangetic Plain: temporal variability and aerosol organic carbon-to-organic mass conversion factor. Sci Total Environ 487:196-205

Taylor SR, McLennan, SM (1995) The geochemical evolution of the continental crust. Review of Geophysics 33(2): 241-265

Urban NB, Slifstein M, Thompson JL, Xu X, Girgis RR, Raheja S, Haney M, Abi-Dargham A (2012) Dopamine release in chronic cannabis users: a [11c] raclopride positron emission tomography study. Biological psychiatry 71(8): 677-683

Viana M, Kuhlbusch T A J, Querol X, Alastuey A, Harrison R M, Hopke P K, Winiwarter W, Vallius M (2008) Source apportionment of particulate matter in Europe: a review of methods and results. J Aerosol Sci 39: 827-849

Yin J, Harrison RM, Chen Q, Rutter A, Schauer J J (2010) Source apportionment of fine particles at urban background and rural sites in the UK atmosphere. Atmos Environ 44(6): 841–851

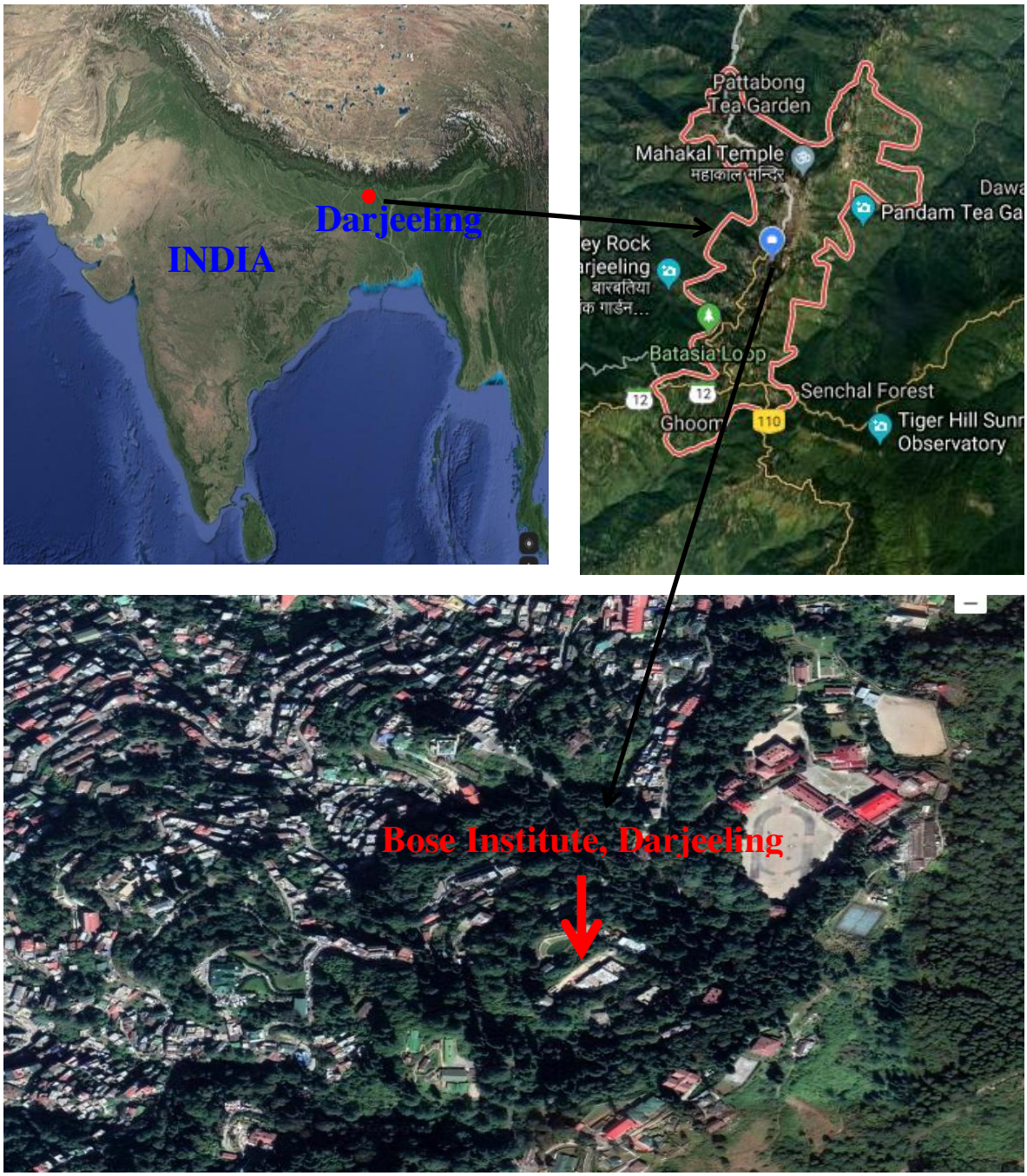

Fig. 1 Map of the observational site (Source: Google maps).

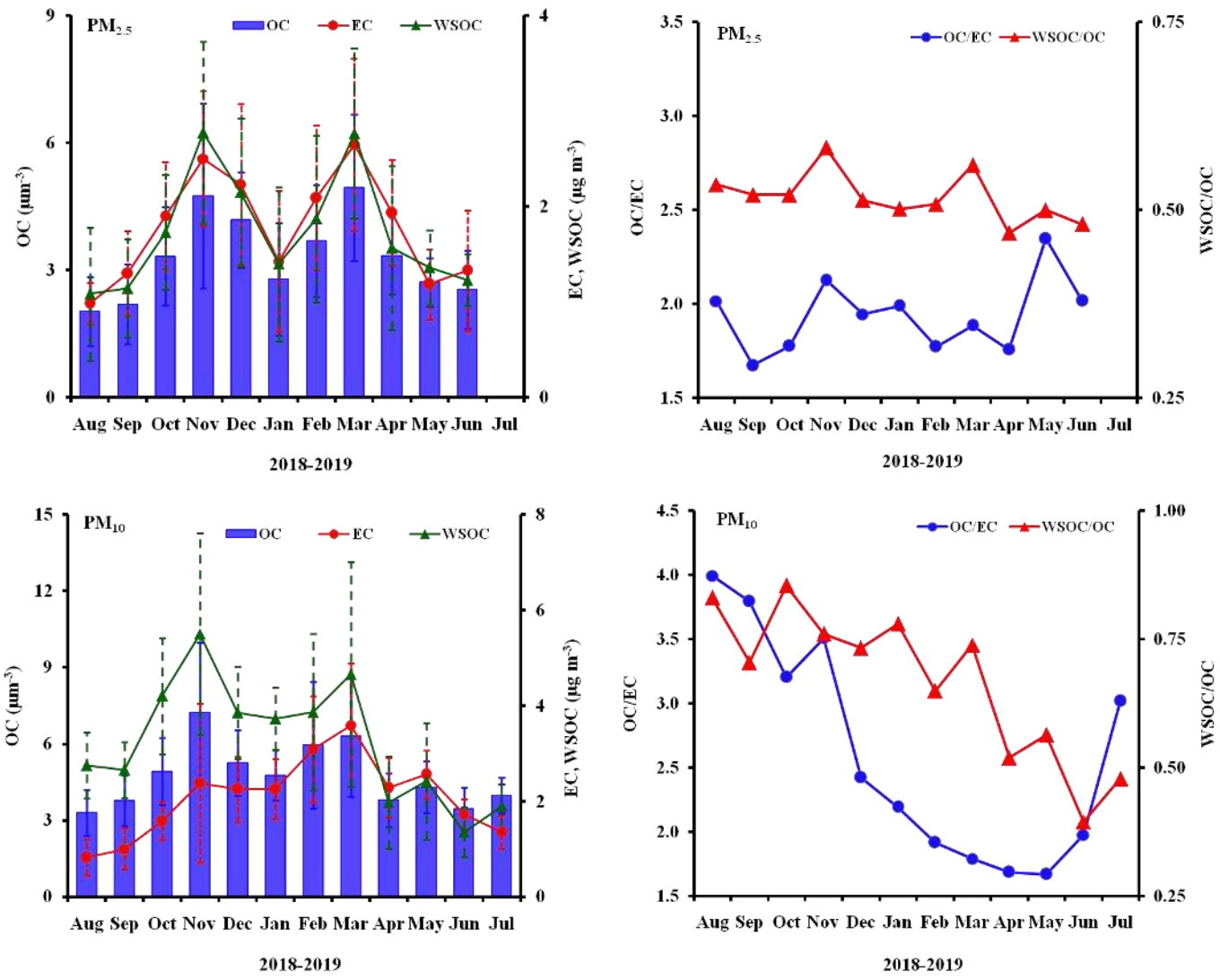

Fig. 2: Monthly average concentrations of OC, EC and WSOC and their mass ratios of $PM_{2.5}$ and PM_{10} at Darjeeling.

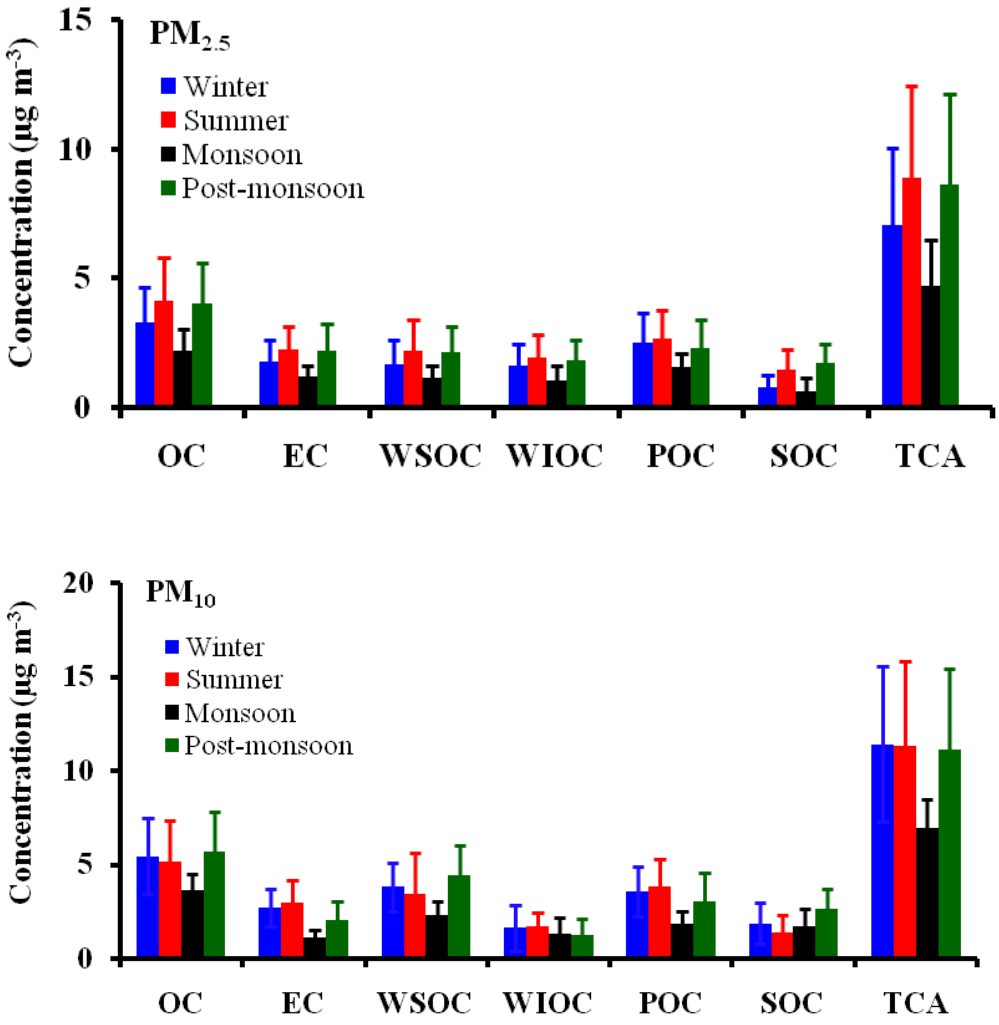

Fig. 3: Average concentrations of carbonaceous species of $PM_{2.5}$ and PM_{10} during winter, summer, monsoon and post-monsoon seasons at Darjeeling.

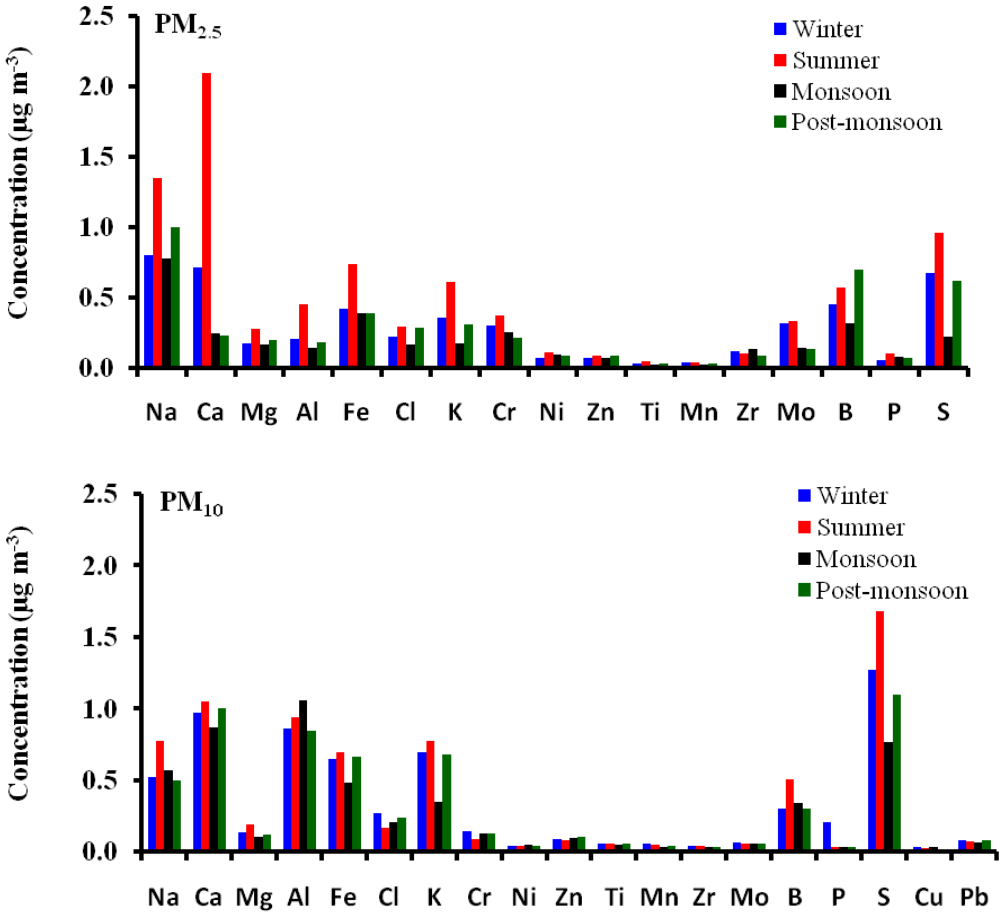

Fig. 4: Average concentrations of major and trace elements in $PM_{2.5}$ and PM_{10} during winter, summer, monsoon and post-monsoon seasons at Darjeeling.

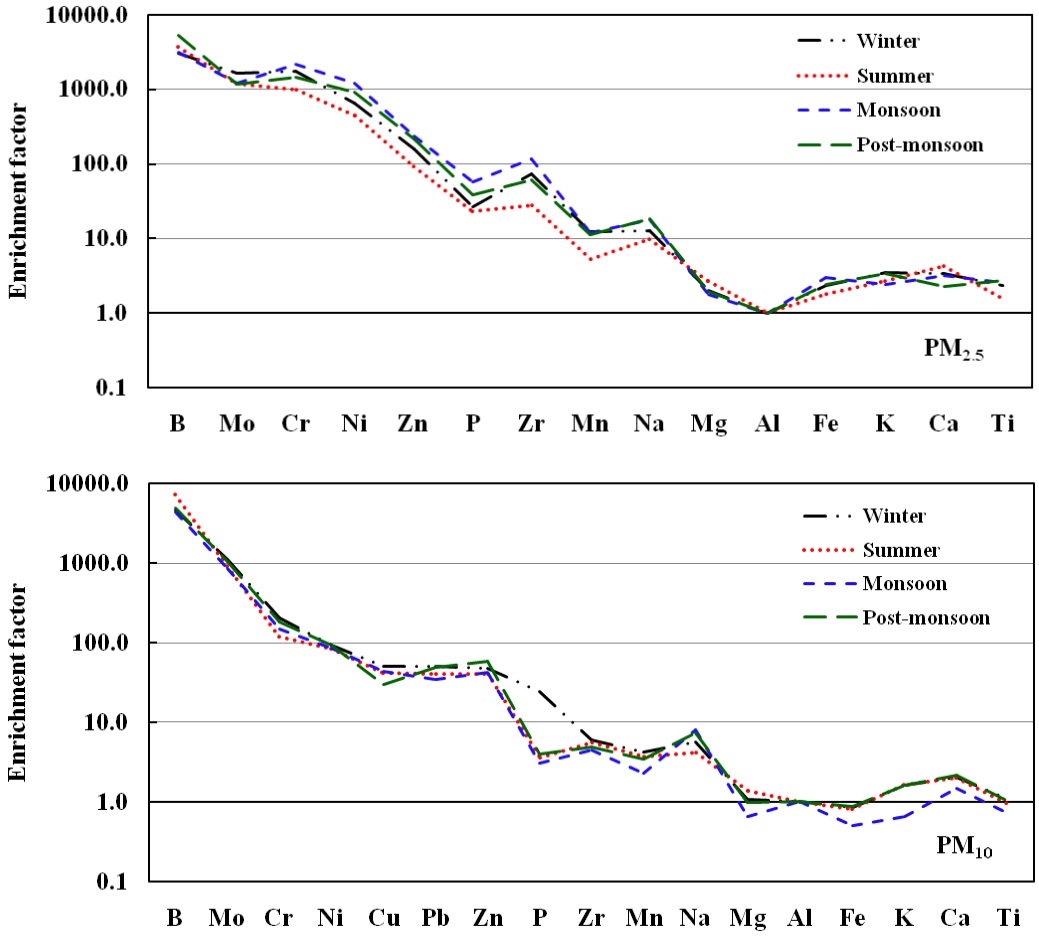

Fig. 5: Enrichment factor of trace elements of $PM_{2.5}$ and PM_{10} during winter, summer, monsoon and post-monsoon seasons at Darjeeling.

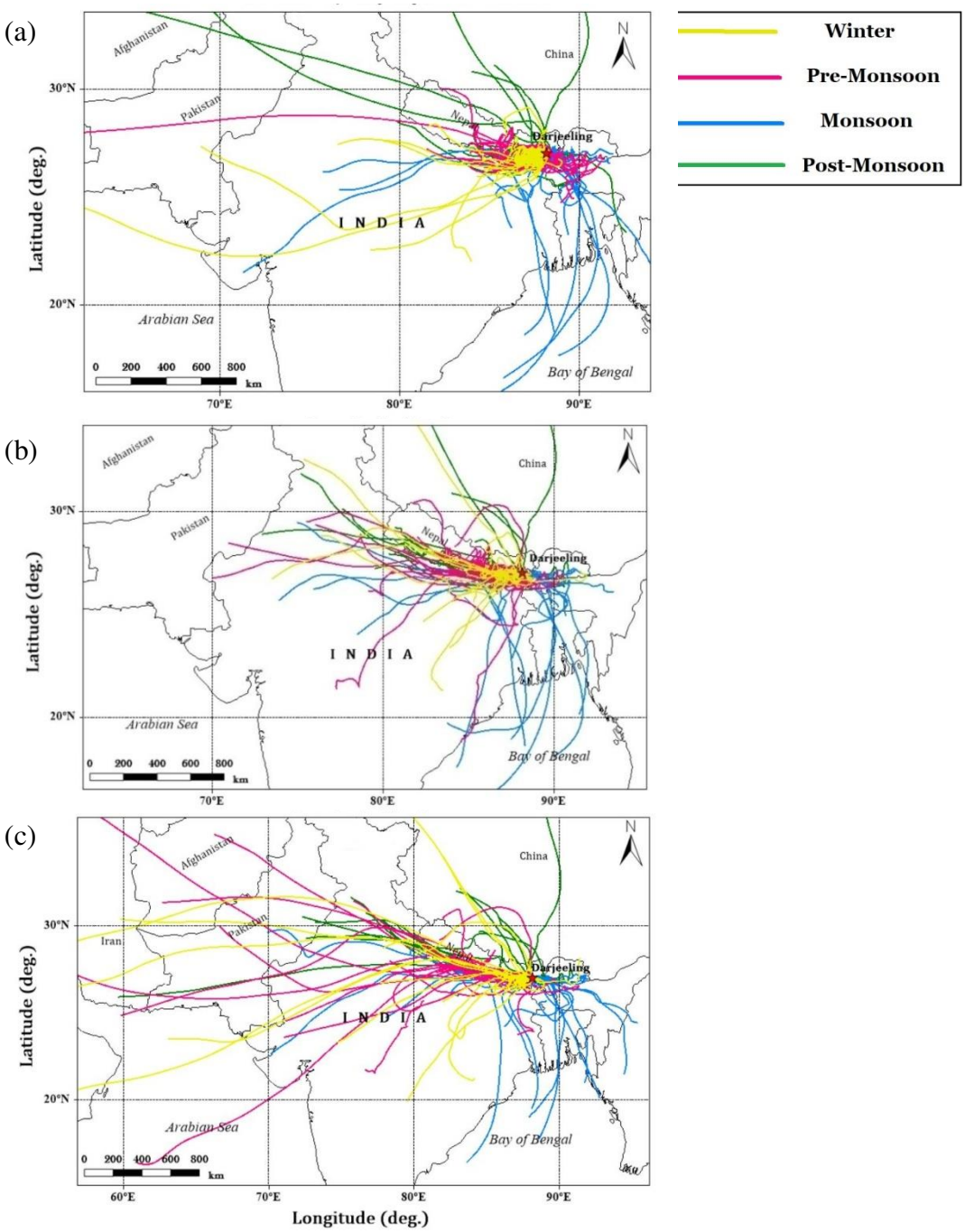

Fig. 6: Five day air mass backward trajectory at sampling site at (a) 100m, (b) 500m, and (c) 1000 m AGL during winter, summer (pre-monsoon), monsoon and post-monsoon seasons.

Table 1. Annual average and seasonal concentrations of $PM_{2.5}$ and PM_{10} and their chemical species (μg m^{-3}) in Darjeeling.

Species	Annual		Winter		Summer		Monsoon		Post monsoon	
	$PM_{2.5}$	**PM_{10}**	**$PM_{2.5}$**	**PM_{10}**	**$PM_{2.5}$**	**PM_{10}**	**$PM_{2.5}$**	**PM_{10}**	**$PM_{2.5}$**	**PM_{10}**
PM	37±12	56±18	31±9	51±17	41±14	64±20	38±8	52±11	40±11.4	55±17
OC	3.56±1.59	5.06±2.03	3.29±1.37	5.43±2.02	4.04±1.67	5.18±2.14	2.21±0.86	3.62±0.87	4.07±1.55	5.69±2.09
EC	1.93±0.93	2.34±1.18	1.80±0.81	2.72±1.01	2.23±0.92	3.01±1.15	1.21±0.43	1.25±0.38	2.19±1.06	2.05±1.02
WSOC	1.88±1.05	3.55±1.75	1.66±0.95	3.80±1.28	2.15±1.19	3.43±2.19	1.14±0.51	2.31±0.77	2.17±0.98	4.44±1.55
WIOC	1.69±0.85	1.51±0.92	1.63±0.85	1.63±1.21	1.94±0.91	1.75±0.68	1.07±0.55	1.31±0.90	1.86±0.78	1.25±0.85
POC	2.35±1.06	3.18±1.31	2.52±1.13	3.56±1.31	2.68±1.10	3.82±1.46	1.57±0.56	1.87±1.31	2.30±1.12	3.07±1.52
SOC	1.19±0.57	2.05±0.98	0.77±0.51	1.87±1.08	1.48±0.76	1.37±0.98	0.64±0.54	1.75±0.91	1.74±0.74	2.62±1.11
TCA	7.63±3.43	10.43±4.25	7.06±2.97	11.41±4.14	8.89±3.54	11.29±4.51	4.74±1.73	6.94±1.55	8.65±3.47	11.15±4.25
Na	1.014±0.392	0.607±0.395	0.801±0.247	0.525±0.343	1.351±0.437	0.776±0.484	0.780±0.272	0.573±0.389	1.002±0.243	0.501±0.239
Mg	0.209±0.075	0.244±0.108	0.172±0.044	0.237±0.066	0.279±0.073	0.191±0.160	0.168±0.052	0.103±0.080	0.195±0.062	0.123±0.041
Ca	0.918±0.813	0.985±0.299	0.716±0.504	0.972±0.178	2.097±0.706	1.051±0.442	0.249±0.213	0.871±0.232	0.229±0.213	1.007±0.182
Cl	0.250±0.147	0.223±0.140	0.221±0.127	0.274±0.126	0.291±0.149	0.171±0.054	0.170±0.050	0.206±0.092	0.283±0.180	0.244±0.118
P	0.078±0.037	0.077±0.034	0.054±0.029	0.212±0.179	0.105±0.026	0.033±0.024	0.081±0.034	0.032±0.013	0.070±0.039	0.033±0.009
S	0.667±0.404	1.260±0.744	0.675±0.382	1.277±0.768	0.956±0.370	1.680±0.744	0.223±0.181	0.771±0.495	0.620±0.284	1.098±0.629
K	0.388±0.224	0.650±0.376	0.360±0.110	0.699±0.295	0.608±0.226	0.774±0.435	0.174±0.050	0.353±0.242	0.307±0.171	0.681±0.346
Al	0.261±0.164	0.922±0.446	0.203±0.104	0.860±0.291	0.454±0.143	0.943±0.661	0.143±0.065	1.061±0.386	0.179±0.068	0.845±0.215
Fe	0.502±0.195	0.635±0.266	0.423±0.141	0.652±0.189	0.737±0.153	0.694±0.381	0.390±0.087	0.482±0.188	0.391±0.067	0.663±0.142
Ti	0.035±0.015	0.057±0.022	0.031±0.009	0.061±0.017	0.047±0.013	0.058±0.031	0.024±0.008	0.049±0.016	0.032±0.018	0.056±0.013
Cr	0.291±0.143	0.122±0.114	0.299±0.102	0.146±0.125	0.372±0.199	0.093±0.014	0.254±0.081	0.132±0.032	0.215±0.074	0.122±0.114
Ni	0.092±0.025	0.084±0.008	0.072±0.012	0.044±0.008	0.110±0.027	0.045±0.006	0.094±0.014	0.049±0.007	0.090±0.021	0.043±0.011
Cu	-	0.028±0.014	-	0.032±0.008	-	0.029±0.005	-	0.034±0.026	-	0.018±0.004
Zn	0.079±0.032	0.092±0.033	0.069±0.035	0.088±0.032	0.088±0.035	0.081±0.027	0.072±0.016	0.097±0.038	0.084±0.031	0.105±0.034
Mn	0.033±0.012	0.048±0.018	0.037±0.010	0.055±0.013	0.037±0.010	0.053±0.016	0.033±0.012	0.036±0.015	0.031±0.015	0.044±0.021
Mo	0.245±0.169	0.060±0.013	0.318±0.236	0.063±0.010	0.337±0.224	0.058±0.013	0.144±0.034	0.061±0.014	0.133±0.028	0.058±0.015
Zr	0.107±0.094	0.061±0.013	0.117±0.099	0.041±0.009	0.102±0.039	0.042±0.012	0.132±0.112	0.038±0.016	0.086±0.026	0.033±0.011
Pb	-	0.076±0.064	-	0.084±0.010	-	0.072±0.069	-	0.069±0.059	-	0.079±0.067
B	0.533±0.389	0.376±0.220	0.455±0.179	0.302±0.174	0.575±0.324	0.510±0.262	0.321±0.096	0.343±0.203	0.702±0.472	0.307±0.132

± Standard deviation (at 1σ)

Table 2. PCA factor loading of $PM_{2.5}$ and PM_{10} samples in Darjeeling, India.

Species	$PM_{2.5}$				PM_{10}			
	Factor 1	**Factor 2**	**Factor 3**	**Factor 4**	**Factor 1**	**Factor 2**	**Factor 3**	**Factor 4**
OC	0.942	0.159	0.482	0.013	0.262	0.912	0.416	0.046
WSOC	0.872	0.095	0.029	-	0.197	0.856	0.174	0.092
EC	0.563	0.138	0.743	0.126	0.182	0.846	0.586	0.186
Na	0.139	0.735	0.031	-	0.851	0.063	0.162	0.142
Mg	0.056	0.832	0.048	0.061	0.909	0.188	0.083	0.098
Ca	0.035	0.877	0.229	0.233	0.935	0.196	0.049	-
Al	0.219	0.898	0.198	0.191	0.860	0.126	0.074	0.368
Fe	0.132	0.852	0.031	0.282	0.882	0.294	-	0.064
Ti	0.383	0.497	0.052	-	0.866	0.257	0.067	0.032
K	0.608	0.588	0.316	0.097	0.628	0.696	0.010	0.055
Cl	0.636	0.137	-	0.394	0.072	0.853	0.389	0.095
P	0.075	0.594	0.160	0.283	0.107	-	0.964	0.068
S	0.574	0.348	0.237	0.361	0.468	0.623	-	0.274
Cr	0.061	0.138	0.235	0.760	0.065	-	0.468	0.674
Ni	-	0.029	0.740	0.396	0.185	-	0.235	0.704
Cu	-	-	-	-	0.109	-	0.425	0.838
Zn	0.281	0.102	0.754	0.467	0.216	0.013	0.530	0.619
Mn	-	0.120	0.436	0.701	0.197	0.056	0.140	0.364
Mo	0.101	0.087	0.891	0.069	-	-	0.037	0.876
Zr	-	-	0.266	0.701	-	-	0.010	0.246
Pb	-	-	-	-	-	0.063	0.273	0.273
B	0.106	-	0.730	0.016	0.523	0.152	0.428	0.428
% Variance	38.5	17.6	11.6	8.7	36.7	16.2	12.4	10.8
Cumulative variance (%)	38.3	55.9	67.5	76.2	36.7	52.9	65.3	76.1
Sources	BB+FFC	Crustal/SD	VE	IE	Crustal/SD	BB+FFC	VE	IE

Extraction method: principal component analysis; rotation method: Varimax with Kaiser Normalization; Eigenvalue >1.00; factor loading ≥ 0.40.
BB: biomass burning; FFC: fossil fuel combustion; SD: soil dust; VE: vehicular emissions; IE: industrial emission.

Figures

Figure 1

Map of the observational site (Source: Google maps).

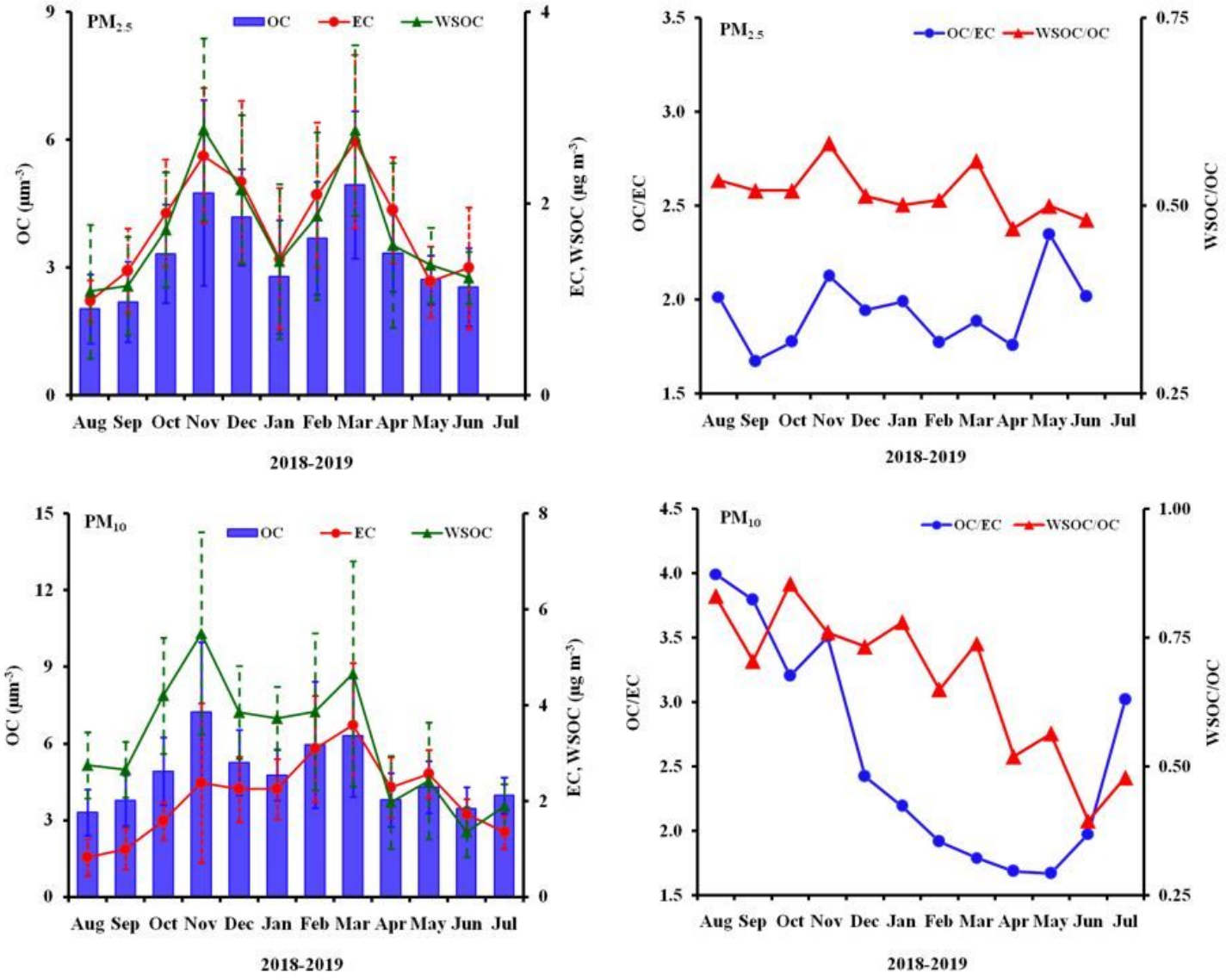

Figure 2

Monthly average concentrations of OC, EC and WSOC and their mass ratios of PM2.5 and PM10 at Darjeeling.

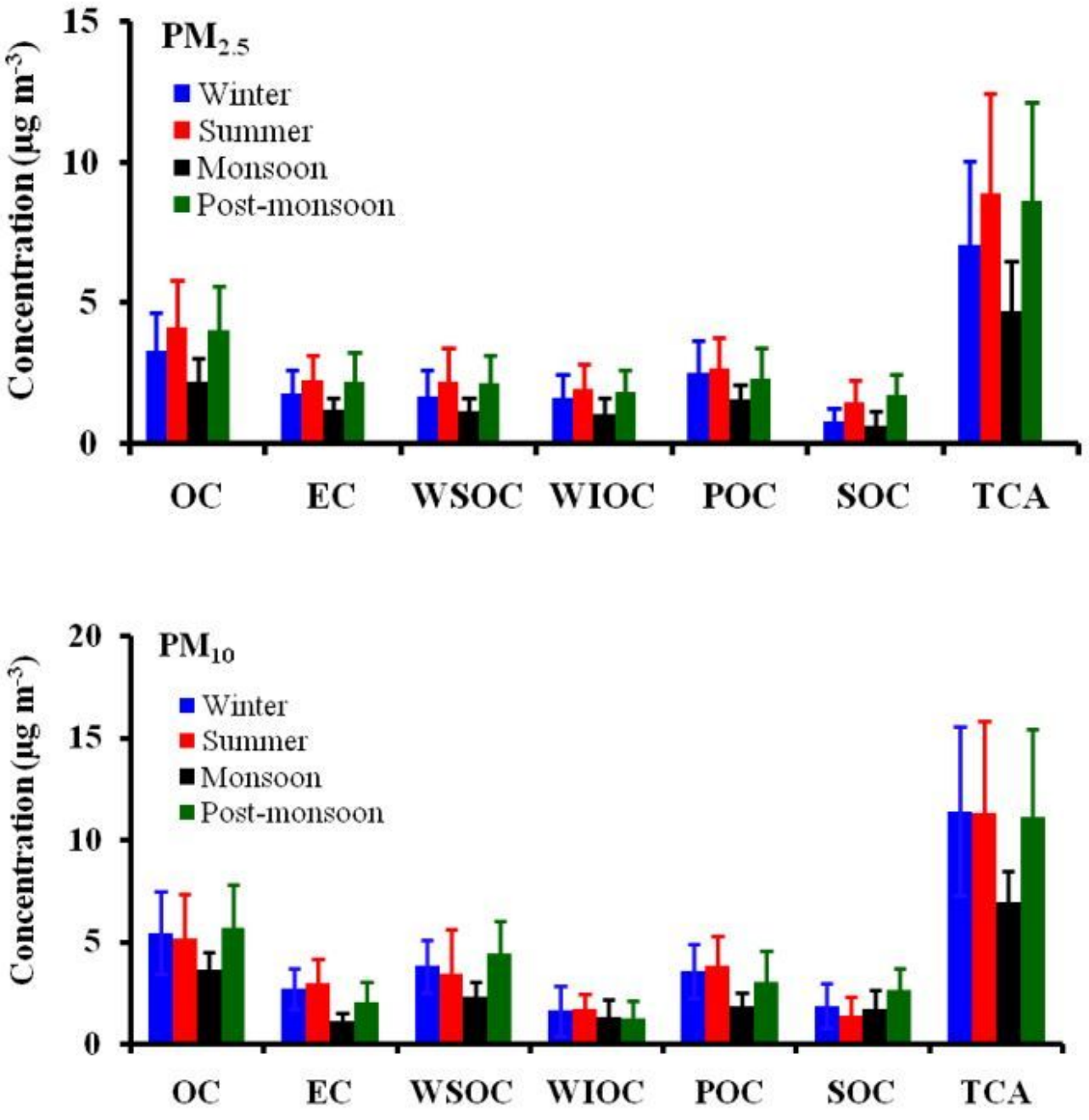

Figure 3

Average concentrations of carbonaceous species of PM2.5 and PM10 during winter, summer, monsoon and post-monsoon seasons at Darjeeling.

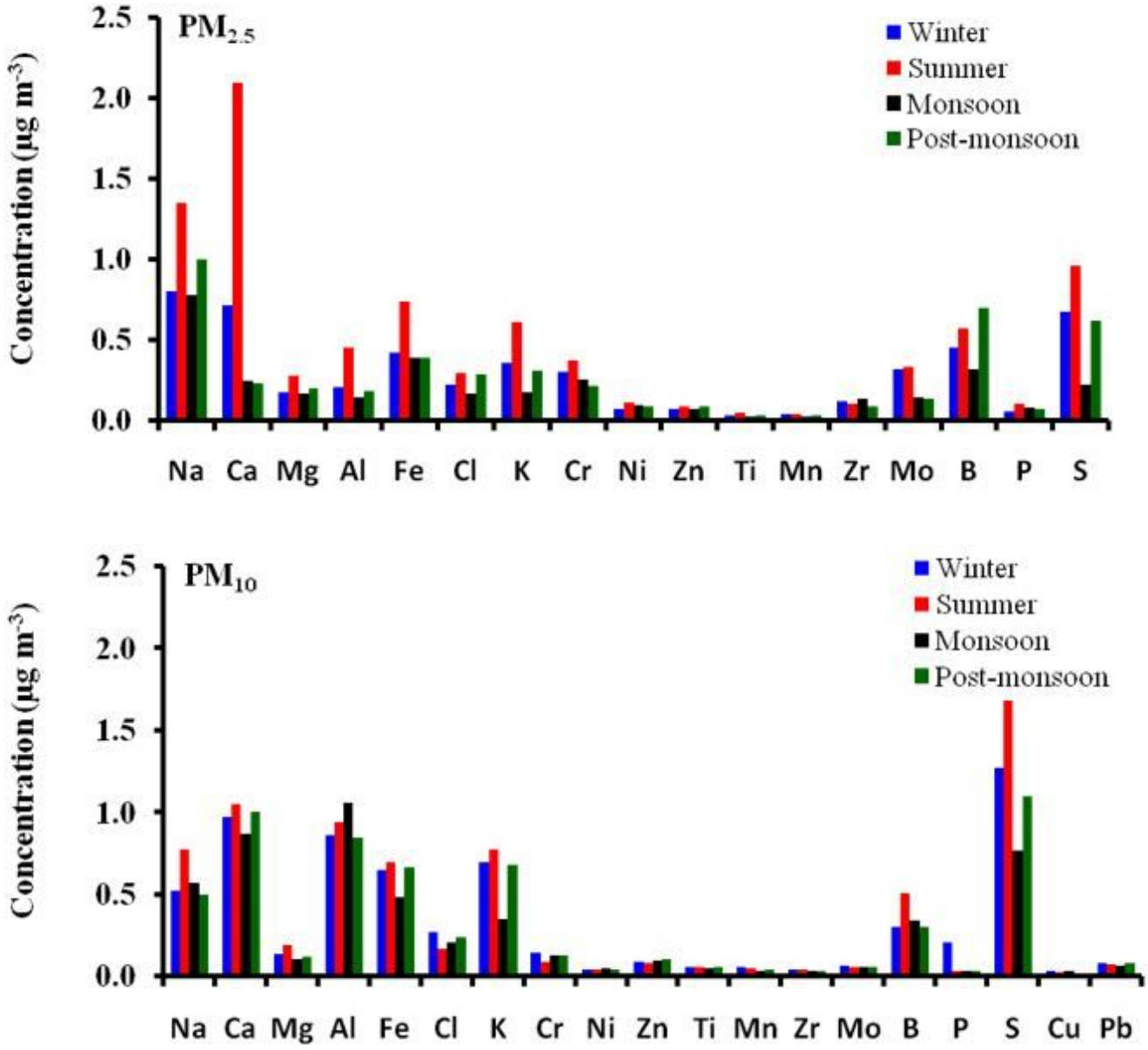

Figure 4

Average concentrations of major and trace elements in PM2.5 and PM10 during winter, summer, monsoon and post-monsoon seasons at Darjeeling

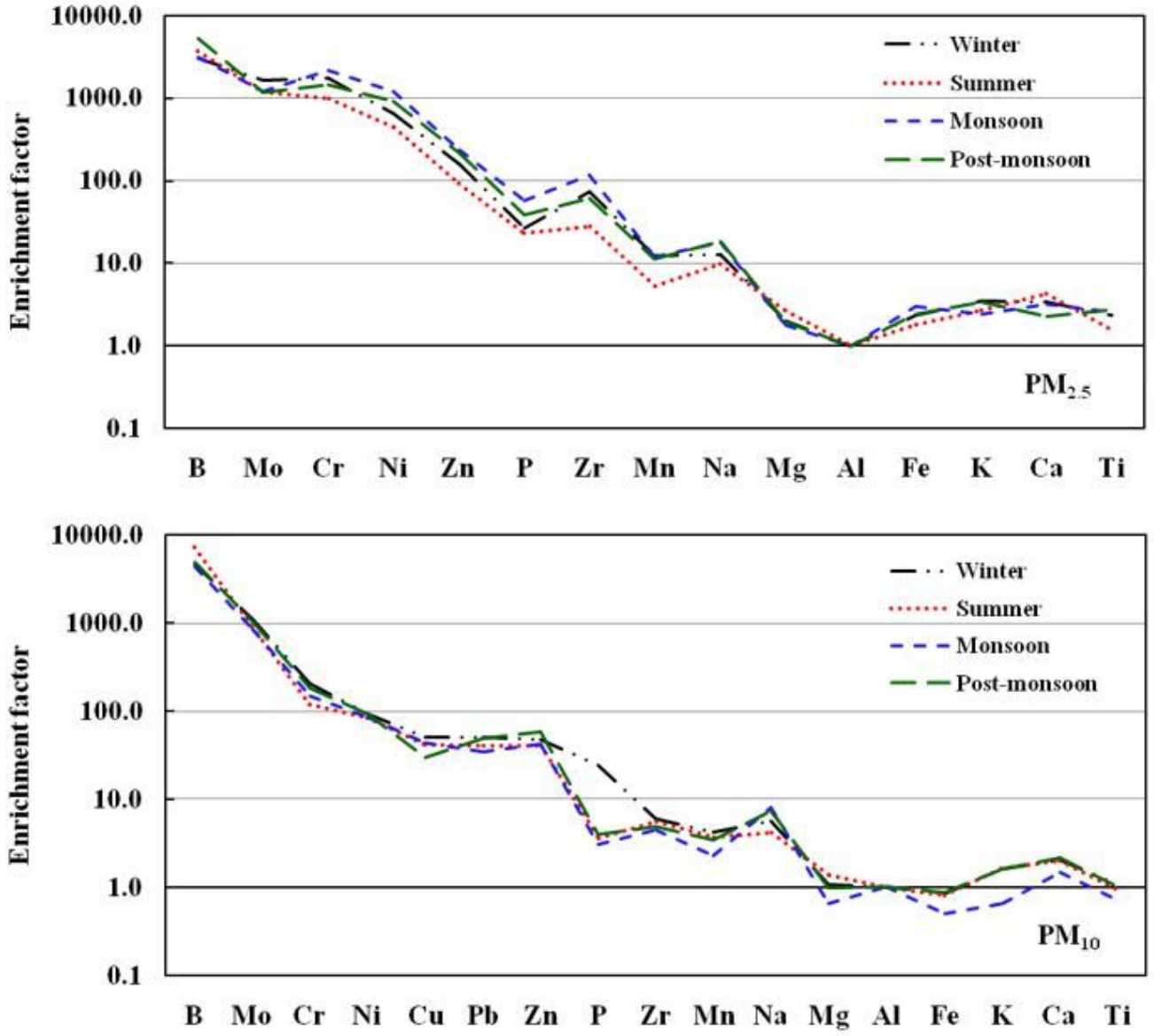

Figure 5

Enrichment factor of trace elements of PM2.5 and PM10 during winter, summer, monsoon and post-monsoon seasons at Darjeeling.

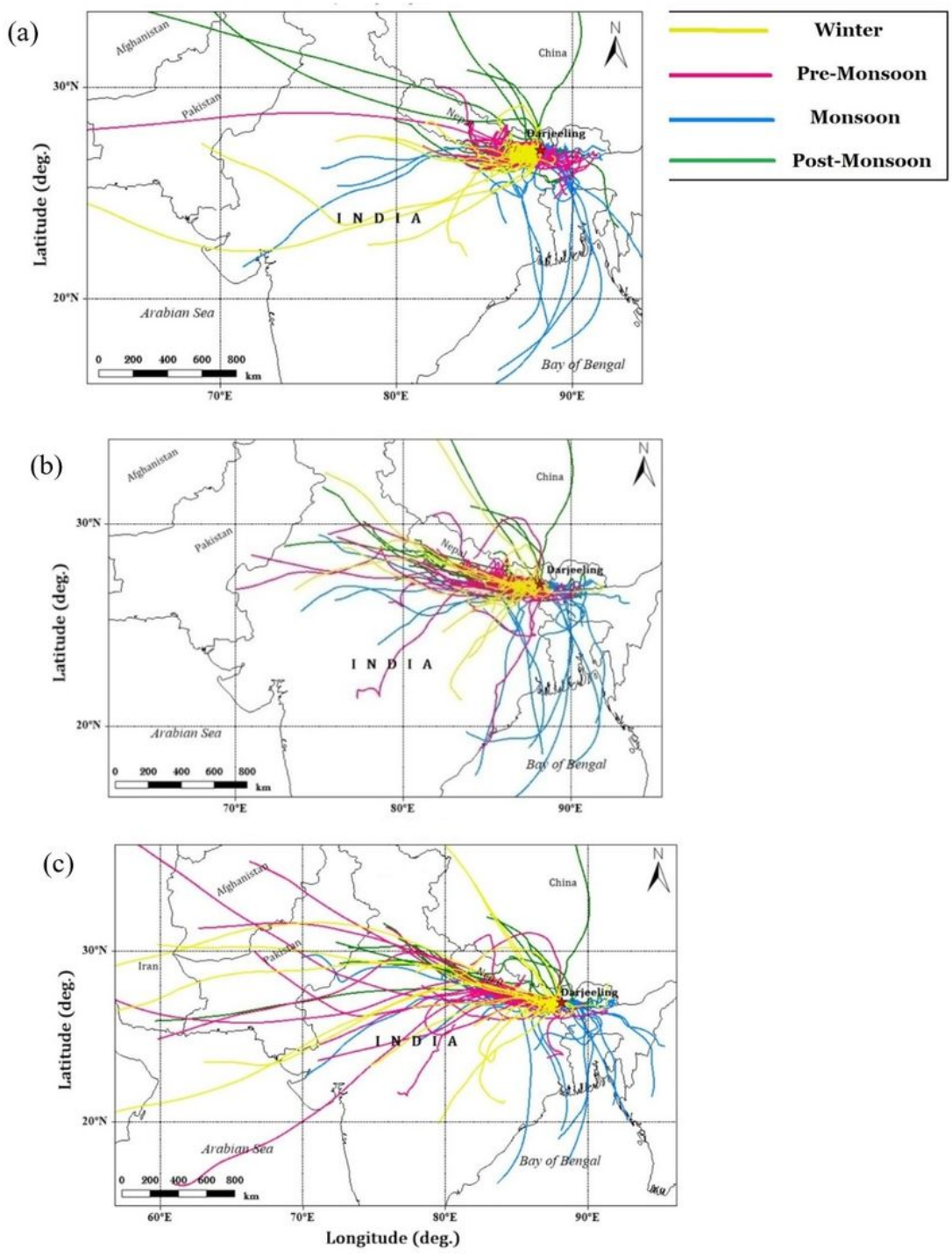

Figure 6

Five day air mass backward trajectory at sampling site at (a) 100m, (b) 500m, and (c) 1000 m AGL during winter, summer (pre-monsoon), monsoon and post-monsoon seasons.

Supplementary Files

This is a list of supplementary files associated with this preprint. Click to download.

- SupplementaryInformation.docx